The metal-non-metal transition in compressed metal vapours

1998 J. Phys.: Condens. Matter 10 11395

(http://iopscience.iop.org/0953-8984/10/49/026)

J. Phys.: Condens. Matter **10** (1998) 11395–11404. Printed in the UK PII: S0953-8984(98)96663-2

The metal–non-metal transition in compressed metal vapours

F Hensel, E Marceca and W C Pilgrim

Institute for Physical Chemistry, Nuclear Chemistry and Macromolecular Chemistry, University of Marburg, Hans-Meerwein-Strasse, 35032 Marburg, Germany

Received 10 August 1998

Abstract. Knowledge of the properties of hydrogen and helium and their mixtures, at temperatures and pressures prevailing in the giant planets is of considerable interest for planetary modelling. In the light of the unfavourable outlook for reliable measurements under these extreme conditions effort has been spent investigating the high-temperature high-pressure properties of fluid metals which are experimentally accessible in the laboratory and which might serve as models for compressed fluid hydrogen. The main emphasis of the paper is on the density dependence of the dynamic structure factor $S(Q, \omega)$ of liquid rubidium which reveals that a monoatomic–molecular transition occurs in the metal–non-metal transition region of the expanded liquid analogous to that suggested to occur in shock compressed hydrogen. Additional emphasis is on new results of the phase behaviour of dilute mixtures of helium in the near critical metal mercury.

1. Introduction

A liquid metal near its triple point is in equilibrium with a low-density, non-metallic vapour. There is, therefore, a metal–non-metal transition that coincides exactly with the liquid–vapour transition, i.e. both the density and the electronic and molecular structures change when a metallic liquid vaporizes.

For example, liquid mercury and caesium near their triple points are considered as normal liquid metals with properties typical of the condensed state. The small changes of basic properties such as the electrical conductivity or magnetic susceptibility on melting [1] show that the electronic structure of the liquid is quite similar to that of the crystalline solid and both liquid and solid can be reasonably well described by the nearly free-electron approximation [1]. This behaviour is usually explained by the fact that the short-range atomic correlations and the atomic density in the liquid near melting are closely similar to those of the crystals. Consequently, the liquid metallic phase is usually treated as a monoatomic state which typifies the solid structure. It is regarded as built-up of single screened ions, each diffusively uncoupled from every other.

In contrast to melting, however, there are substantial changes in the nature of bonding upon evaporation. At sufficiently low densities, in the vapour phase, the valence electrons occupy spatially localized atomic or molecular orbitals. In this state many caesium atoms form chemically bound dimers with a dissociation energy of 0.45 eV, whereas in the vapour phase of mercury, chemically bonded dimers do not form because the ground state of the mercury atom arises from a closed shell electronic configuration which by itself cannot form an appreciable bond owing to the inert character of the $6s^2$ shell. The interaction potential

0953-8984/98/4911395+10$19.50

between two mercury atoms is thus generally regarded as acting between highly polarizable closed-shell systems involving very little electronic density migration from the partners, in a similar way to noble gas atoms. In this sense, mercury vapour has been denoted 'pseudo-helium' [2], while the vapour of the alkali metal caesium resembles hydrogen [3].

However, this description applies only to conditions near the triple point and whether the liquid–vapour phase change is always and necessarily accompanied by a metal–non-metal transition, even up to the liquid vapour critical point, is one of the points at issue [4]. It almost certainly is not the case in mercury [5] but may be so in caesium, rubidium and potassium [6, 7]. Another point at issue is whether chemical bonding plays a significant role in liquid alkali metals as the density is lowered towards the critical density.

Renewed interest in this question is motivated by the exciting progress in the search for metallic hydrogen which has come from the recent shock wave experiments of Weir *et al* [8]. They found a highly conducting state of hydrogen (and also deuterium) at high temperatures and in a pressure range above 1.4 Mbar. Their measurements of the electrical conductivity at these conditions showed values of about 2000 Ω^{-1} cm^{-1} comparable with those for expanded liquid caesium and rubidium [6, 9, 10]. Weir *et al* [8] interpreted their findings in terms of the existence of H_2 molecules within the highly conducting fluid phase. It has so far, however, not been possible to investigate the structural properties of fluid hydrogen at the extraordinarily high temperatures and pressures prevailing in the shock wave experiment in order to prove whether the pairing character persists in the highly conducting state. This has, therefore, stimulated a number of theoretical studies [11–13] which suggest that significant concentrations of neutral dimers and dimer ions exist under these conditions. Given the close similarity in their atomic structure, an alternative experimental approach is to investigate the structural properties at high temperatures of the experimentally accessible fluid alkali metals, which may serve as models for the metallization of shock compressed hydrogen.

It goes without saying that the metallization of hydrogen at high temperatures and pressures has implications for affecting the thermodynamics of hydrogen–helium mixtures which are of considerable interest for planetary modelling. Unfortunately, until now it has not been possible to investigate the phase behaviour of these mixtures at the extreme conditions where hydrogen becomes metallic. In the light of the unfavourable outlook for such measurements, effort has been spent experimentally investigating phase diagrams of other fluid metal–helium mixtures in the metal–non-metal transition range of the metal component which might serve as models for the hydrogen–helium system. Of special interest in this respect is the mercury–helium system because mercury has a liquid–vapour critical point and a metal–non-metal transition density which lie within the range of experimentally accessible conditions.

2. Expanded alkali metals

The metal–non-metal transition and its relation to thermodynamic phase behaviour has been studied for mercury [5], caesium [9], rubidium [6], and potassium [6] because they have critical points that lie within the current limits of static temperatures and pressures available in the laboratory (see table 1).

The most transparent experimental parameter relevant to this interrelation is perhaps the variation of the electrical conductivity σ with pressure and temperature. For example, the variation of σ of caesium with pressure shows a sharp drop close to the critical point (figure 1(a)). This indicates that the transition from liquid to vapour has a strong effect on the electronic structure, and *vice versa*. However, although the conductivity varies rapidly,

Table 1.

Metal	T_c (K)	P_c (bar)
Hg	1751	1673
Cs	1924	92.5
Rb	2017	124.5
K	2280	161.0

there is no indication of a discontinuous first-order electronic phase transition except across the liquid–vapour co-existence curve. The thermodynamic phase transition separates the low-conductivity elemental vapour from the highly conducting metallic liquid.

Taken as a group, the alkali metals exhibit very similar electrical conductivities. At the critical point, the conductivity is about 100 Ω^{-1} cm^{-1} for each of the three alkali metals (potassium, rubidium and caesium) that have been studied experimentally in the critical region [6]. Also the results for divalent mercury are qualitatively similar to those of the alkali metals except that mercury conductivity near the critical point is about 100 times smaller. This indicates that the behaviour of the electronic properties of metals is not universal.

There is also a close correlation between the behaviour of the conductivity (figure 1(a)) and the density (figure 1(b)) as a function of pressure. This shows that density is the dominant thermodynamic variable governing the metal–non-metal transition in mercury and the alkali metals. In this respect the metal–non-metal transition is similar to the continuous transition to the highly conducting state observed in the high-temperature experiment on shock-compressed fluid hydrogen [8]. This is immediately evident from figure 2 which displays the electrical conductivity for compressed fluid hydrogen and the expanded fluids mercury, rubidium and caesium measured at comparable supercritical temperatures (1800–4000 K) over a range of atom densities N. All four fluid elements undergo a density-induced, continuous transition from a low conductivity to a highly conducting state ($\sigma(0) \sim 2000\ \Omega^{-1}$ cm^{-1}). However, the density at which this occurs for fluid hydrogen is about 100 times that required for rubidium and caesium and about 20 times that required for mercury. It is self-evident that the differences in the transition densities are related to characteristic atomic properties. One such property, for example, is the radius of the principal maximum in the charge density of the ns valence orbital a^* which enters into the celebrated Mott criterion [14]. The relatively small value of a^* for atomic hydrogen (0.529 Å) then indicates that high densities at pressures of several megabar are required for the transition to metallic hydrogen. In contrast, the high-a^* values of rubidium (2.29 Å), caesium (2.52 Å), and mercury (1.13 Å) ensure that they are metallic at normal conditions, and that they transform to an elemental state of low conductivity when they are expanded to lower density at high temperatures (under pressures of about 100 to 1000 bar).

Although the characteristic transition densities for the alkali metals are considerably less than for hydrogen, with respect to the density induced transition to the metallic state the fluids are expected to be closely similar. We have seen earlier that there are hints [8, 11–13] for fluid hydrogen that the tendency of the structure to dimerize persists up to the densities and temperatures prevailing in the shock experiment. The question then emerges whether dimers and other cluster species can be detected by structural measurements in expanded fluid alkali metals. Naturally to pose this question is to ask further what is the relation of dimer formation to the metal–non-metal transition? The underlying view [15, 16] is that the transition in hydrogen and the alkali metals may begin with metallization of the diatomic

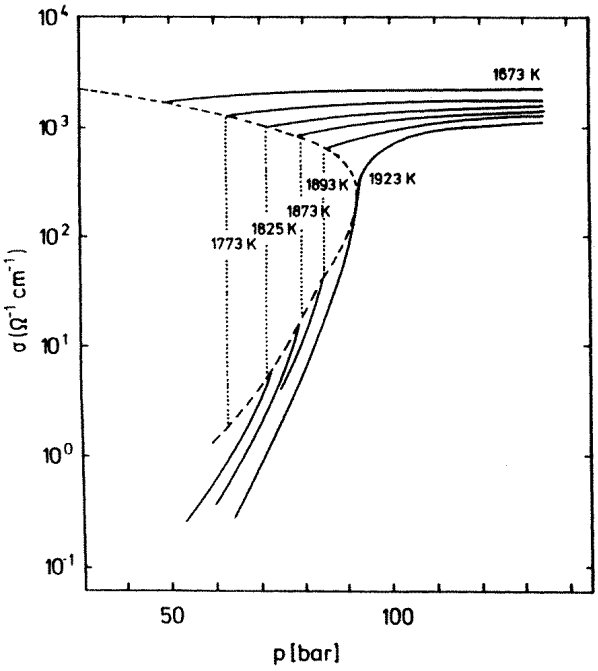

(a)

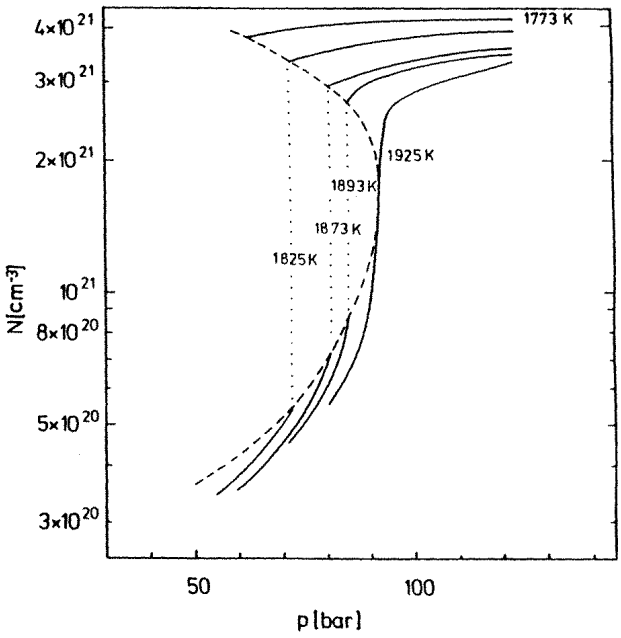

(b)

Figure 1. (a) Electrical conductivity isotherms of fluid caesium at subcritical and supercritical temperatures as a function of pressure in the near-critical region. (b) Equation-of-state data of fluid caesium at subcritical and supercritical temperatures as a function of pressure in the near-critical region.

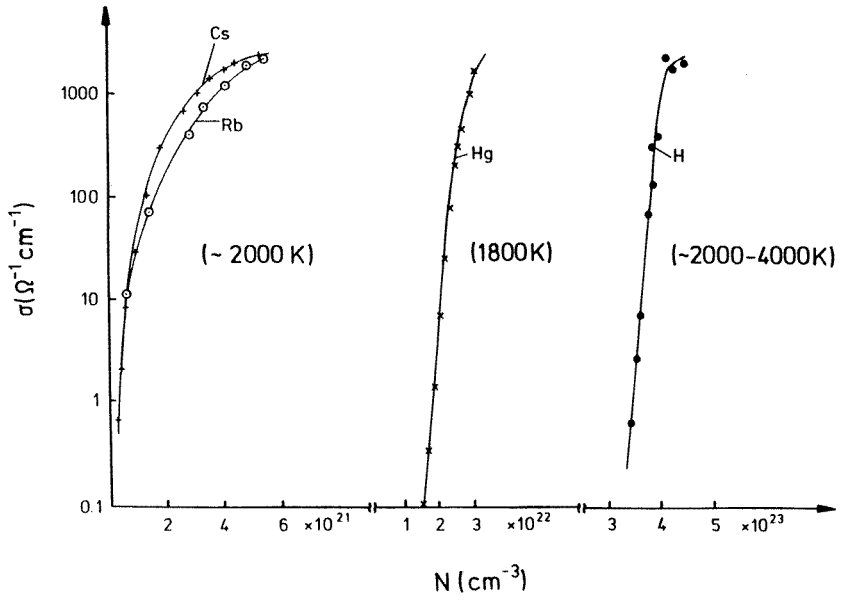

Figure 2. DC electrical conductivity of fluid caesium, rubidium, mercury, and hydrogen against atomic density at supercritical temperatures.

system by an overlap of the molecular valence and conduction bands. This is followed at higher fluid density by a gradual transition into a monoatomic state.

Thus, while liquid alkali metals might be regarded as monoatomic near the melting point, the viewpoint might be rather different for the lower density liquid regime where dimers of higher clusters can be the appropriate structural subunits. The dimer molecules present in the vapour might well survive the passage to metallic liquid [3].

The problem that throughout the liquid range of an alkali metal the dynamic units can change significantly with density and temperature, i.e. that vestiges of dimers can persist in the lower-density range of the liquid, has stimulated neutron-scattering measurements of the static structure factor $S(Q)$ of caesium and rubidium [17, 18]. The data obtained show that the dominant effect of thermal expansion of the liquid is a reduction of the average coordination number (thermal hole formation), while the average interparticle distance grows only very little. However, within standard approximations of theoretical descriptions and within experimental uncertainties, $S(Q)$ data do not provide a clear-cut answer to the question posed earlier. The problem is that quite different views of the microscopic structure of expanded liquid alkali metals are possible to describe $S(Q)$ reasonably well.

A more interesting insight into the question of whether remnants of the diatomic unit, present in the dense vapour phase of alkali metals, can survive condensation to the liquid state can be obtained by examining recent coherent inelastic neutron-scattering spectra for liquid rubidium [16, 19] which extend nearly to the critical region. From the early work of Copley and Rowe [20] it is known that rubidium near its melting point at 320 K unlike dense Lennard-Jones (inert-gas) systems, exhibits distinct longitudinal collective excitations up to relatively high Q-values. The measured dispersion relation resembles very much that of longitudinal phonons in crystalline rubidium. The more recent measurements of $S(Q, \omega)$ for expanded liquid rubidium [16, 19] show that these collective excitations can be observed over a very wide temperature range (up to at least 1673 K) in this metal.

The comparison of these results with molecular dynamics calculations [21, 22] supports the view that liquid rubidium at a temperature of 1673 K and a density of $\rho = 0.87$ g cm^{-3} (the corresponding atom number density is 6.1×10^{21} cm^{-3}) is still basically monoatomic and the screened forces typical for metallic binding still control the liquid dynamics under these conditions. However, this is no longer true when the temperature is increased still further and evidence of intramolecular vibrations appears. This is immediately evident from a glance at figure 3 which displays the longitudinal current correlation function $J_1(Q, \omega) = (\omega^2/Q^2)S(Q, \omega)$ for $Q = 1.3$ Å^{-1} at 1873 K. The liquid density at this point is 0.61 g cm^{-3} (the corresponding number density N is 4.3×10^{21} cm^{-3}). Three peaks can be clearly identified as resulting from excitations at 3.2 meV with higher harmonics at 6.4 and 9.6 meV. This feature was assigned to excitation of local harmonic oscillations in the environment of their neighbouring atoms in the liquid.

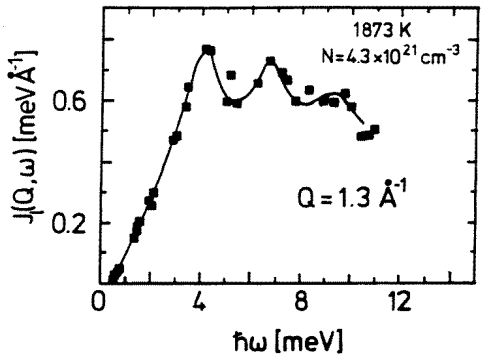

Figure 3. Experimentally determined current correlation function for liquid rubidium $J_l(Q, \omega) = (\omega^2/Q^2)S(Q, \omega)$ at $Q = 1.3$ Å^{-1} at $T = 1873$ K and $N = 4.3 \times 10^{21}$ cm^{-3}. The full curve is a guide for the eye.

The measured excitation energy of 3.2 meV is surprisingly close to that calculated for Rb_2 molecules on a simple cubic lattice [16]. These are calculations for the total energy of expanded lattices of monoatomic Rb and Rb_2 dimers using density functional theory in the local density approximation. They were made for a system of Rb atoms in a body-centred cubic lattice (BCC) and for diatomic molecules in a simple cubic lattice (SC). To create the diatomic solid two atoms in the BCC unit cell were moved towards one another forming a simple cubic lattice (SC). The dimer bond length in the molecular lattice was varied to minimize the total energy. Below a density of 0.9 g cm^{-3}, which corresponds to an N of 6.3×10^{21} cm^{-3}, the SC Rb_2 lattice has the lowest energy.

The vibron energy and dissociation energy were obtained by displacing the bond length from its equilibrium value R_0 and calculating the change in energy $E(R - R_0)$. These data were then fitted to a Morse potential. The calculations predict that the vibron and dissociation energy decrease with increasing density from their gas-phase value to zero near $N = 6.3 \times 10^{21}$ cm^{-3}. Such a decrease in vibron energy with increasing density is a well established feature found in optical studies on solid molecular hydrogen [23]. Thus, the results of the calculation support the view that rubidium, which is stable as a diatomic molecule at low density, may undergo a density-induced molecule-to-metal transition at $N = 6 \times 10^{21}$ cm^{-3} which is analogous to that which is suggested to occur in shock compressed hydrogen [8].

This view is also consistent with a recent statistical mechanical study of fluid rubidium at conditions along the liquid–vapour co-existence curve [24]. This study predicts that the highest density at which dimers appear is $N = 6 \times 10^{21}$ cm^{-3}; it shows also that in the region of 4.3×10^{21} cm^{-3} the combined concentration of Rb_2 and Rb_2^+ is the order of 40%. The conductivity calculated within the framework of this partially ionized plasma model [25] is in very good agreement with the experimental values displayed in figure 2.

3. Phase equilibria in dilute mercury–helium mixtures

The possible importance of limited solubility of helium in hydrogen for planetary modelling has been recognized for a long time [26]. Helium is known to have limited solubility in molecular hydrogen at low pressure [27, 28] and it could be valuable to extend the understanding of this mixture to the extraordinary high temperatures and pressures in giant planet interiors, indeed, even to the limits of the stability of the molecular phase of hydrogen. It is unfortunate, however, that precise experimental phase diagrams have been obtained only up to kilobar pressures [27]. As discussed in the preceding section hydrogen has been found to be a fluid metal only at pressures above about 1.4 Mbar and 3000 K. Thus, there is a large gap between the range of existing phase diagrams and conditions that are relevant to the extremes of temperatures and pressures found in astrophysical settings.

This has, therefore, stimulated theoretical studies of the metallic-hydrogen–molecular-helium system [29–31]. To proceed beyond the range of existing data, theorists need, in particular, reliable knowledge of the interaction of neutral helium with the itinerant electronic states of metallic hydrogen. It becomes, therefore, interesting to study the high temperature—high pressure phase diagrams of other metal–helium mixtures that are experimentally accessible and which can serve as models for the metallic-hydrogen–molecular-helium system. Of special interest in this respect is fluid divalent mercury which experiences at sufficiently high density a band overlap transition to a metallic state not unlike that of diatomic hydrogen at pressures that are relevant to planetary interiors.

For pure fluid mercury, properties such as the electrical conductivity, thermopower, Hall coefficient, Knight shift, optical reflectivity and optical absorption have been studied as functions of temperature and pressure up to and beyond the critical point [5]. Each of these properties exhibits remarkable variation with density. For example, the dc conductivity decreases by more than seven orders of magnitude as the density is reduced from $N = 4.1 \times 10^{22}$ cm^{-3} to 0.6×10^{22} cm^{-3}.

A comparison of the conductivity, Hall coefficient and the Knight shift shows that for densities down to about $N = 3.3 \times 10^{22}$ cm^{-3}, the properties of mercury can be described by the nearly free electron theory of metals, but with further decreases in density, the metallic properties rather gradually diminish and for $N = 2.7 \times 10^{22}$ the properties become compatible with the opening of an energy gap which widens rapidly when the density decreases further. Ultimately, in the limit of very low density, the gap must approach the ionization potential (10.4 eV). Thermal excitation of charge carriers decreases rapidly once the gap opens and as the gap continues to widen, fluid mercury evolves to a dense, partially or weakly ionized gas [5] not unlike that of shock compressed hydrogen for atomic densities smaller than $N = 5 \times 10^{23}$ cm^{-3} and conductivities smaller than 2000 Ω^{-1} cm^{-1} (see figure 2).

In pure mercury, equilibrium between two fluid phases is limited to the vapour–liquid equilibrium, and above the critical temperature the density can be continuously varied at will, allowing us to determine the density at which the fluid becomes a metal or a non-metal. The situation is quite different, however, as soon as a second component is added

to pure mercury. For a two-component system, the equilibrium region where two fluid phases coexist is not necessarily limited to temperatures below the critical temperature of the less volatile component. On the contrary, in binary systems with poorly attractive or even repulsive interactions between the two component fluid–fluid phase separation occurs above the critical points of the pure components.

It is well known that the solubility of helium in fluid metallic systems such as mercury is extremely small at high densities, because the energy required to immerse a helium atom in the metallic system is very high and phase separation occurs at very low concentrations of helium in the metal. It is essentially the strong repulsive interaction between the neutral helium atom and itinerant states of the dense free-electron gas [29] which has been proposed as the microscopic basis of this demixing. Since there is a close relationship between the metal–non-metal transition and the vapour–liquid transition, it is expected that demixing in the mercury–helium system reaches up to the supercritical region of pure mercury.

Figure 4 shows the three-dimensional phase behaviour expected for the mercury–helium system in schematic form. This diagram includes the vapour pressure curves and liquid–vapour critical points of the pure components mercury and helium in their respective $x = 1$ planes. A two-phase coexisting surface is expected to appear folded along the vapour pressure curve of mercury and then along the critical line denoted cl which extends up to very high pressures and temperatures. This expectation has been confirmed by measurements of the pressure–density–temperature–composition diagram at very low helium concentrations and at pressures close to the critical pressure of pure mercury. The experiments extend up to 1800 K and to pressures up to 3300 bars. The p–T–x phase equilibrium surface obtained is displayed in figure 5. It is indeed qualitatively like that shown schematically in figure 4. The critical line starts at the critical point of pure mercury ($T_c = 1751$ K, $p_c = 1673$ bar) and moves directly to higher temperatures and pressures as the helium mole fraction X_{He} increases. Figure 5 illustrates two isotherms together with representative tie lines which connect the coexisting phases ($'$) and ($''$). The phase diagram is straightforward and requires little comment.

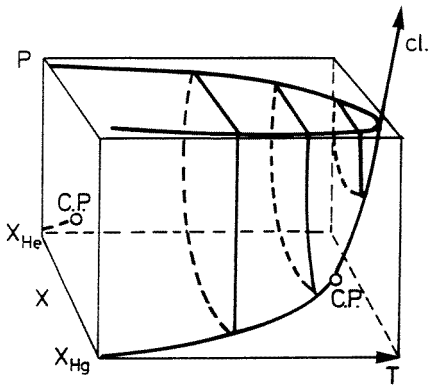

Figure 4. Schematic three-dimensional p–T–x phase diagram for the binary fluid–fluid mercury–helium system. The curves terminating in $x_{Hg} = 1$ and $x_{He} = 1$ represent the vapour pressure curves of the two pure components. The curve 'cl' is the critical line extending from the critical point of pure mercury.

Since density measurements have also been made on the mercury–helium system it is possible to obtain the N–T–x equilibrium phase surface. Figure 6 shows two isothermal

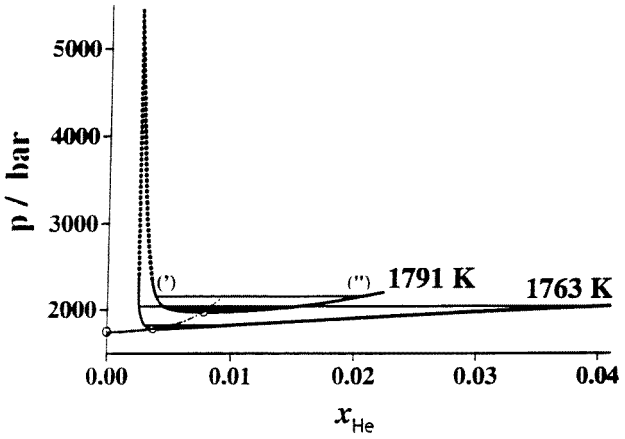

Figure 5. Representative (p, x) isotherms for mercury–helium mixtures. The critical line is shown dot-dashed. It connects the critical points (open circles).

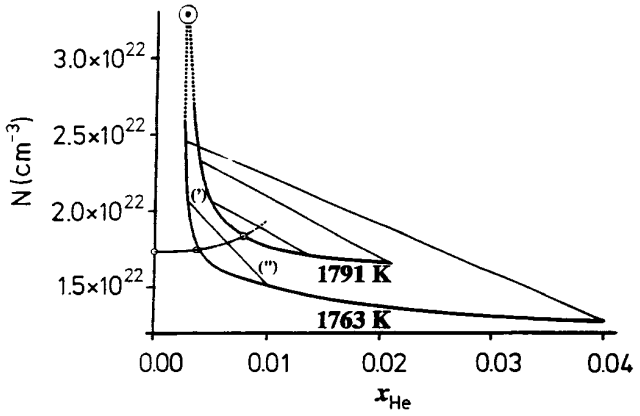

Figure 6. Isotherms in the density N–composition x plane of the mercury–helium phase diagram at 1763 K and 1791 K. The dot-dashed curve is the critical line connecting critical points (open circles); heavy full curves represent solubility curves and are extrapolated (dashed curves) to $N' = 3.3 \times 10^{22}$ cm^{-3}.

(N–x_{He}) sections of the phase diagram. The two-phase region is located above the helium solubility curves of phases ($'$) and ($''$) on the left- and on the right-hand side of the critical line, respectively. Representative tie lines connecting coexisting phases are shown in the figure and the corresponding values of the equilibrium variables are given in table 2. Experimental data (thick full curves) show that the helium solubility in the denser phase ($'$) decreases monotonically as the density increases along the metal–non-metal transition region of Hg. The N–x_{He} data trend has been used to extrapolate the solubility isotherms to $N' = 3.3 \times 10^{22}$ cm^{-3}, where most of the properties of Hg are well described by the free electron model.

The solubility at that density (circle in figure 6) was estimated from the effective immersion energy for a helium atom in a free electron gas whose density corresponds to divalent mercury at the atom density of 3.3×10^{22} cm^{-3} [33]. The good agreement

Table 2. Critical points and tie lines connecting phases (′) and (″) shown in figure 6.

T (°C)	p (kbar)	x'_{He} (at.%)	x''_{He} (at.%)	N' (cm^{-3})	N'' (cm^{-3})
1490	1.78	0.37	0.37	1.75×10^{22}	1.75×10^{22}
1490	1.82	0.30	1.01	2.07×10^{22}	1.72×10^{22}
1490	2.04	0.26	4.00	2.47×10^{22}	1.28×10^{22}
1518	1.97	0.78	0.78	1.84×10^{22}	1.84×10^{22}
1518	2.01	0.50	1.37	2.07×10^{22}	1.72×10^{22}
1518	2.15	0.39	2.09	2.34×10^{22}	1.66×10^{22}

between the calculated solubility and that extrapolated from the trend of the experimentally determined one supports the suggestion of Stevenson [33] that at not too high electron densities phase separation is caused predominantly by the structure-independent interaction of the electron gas with the repulsive interaction of the neutral helium atom.

References

[1] Shimoji M 1977 *Liquid Metals* (London: Academic)
[2] Pyykkö P 1978 *Adv. Quantum Chem.* **11** 353
[3] Ashcroft N W 1990 *Nuovo Cimento* **12** 597
[4] Landau L and Zeldovitch G 1943 *Acta Phys. Chem. USSR* **18** 1940
[5] Hensel F 1995 *Adv. Phys.* **44** 3
[6] Freyland W 1981 *Comment. Solid State Phys.* **10** 1
[7] Hensel F and Uchtmann H 1989 *Rev. Phys. Chem.* A **40** 61
[8] Weir S T, Mitchell A C and Nellis W J 1996 *Phys. Rev. Lett.* **76** 1860
[9] Hensel F, Stolz M, Hohl G, Winter R and Götzlaff W 1991 *J. Physique Coll.* C **5** suppl 1, 191–205
[10] Hensel F and Edwards P P 1996 *Chem. Eur. J.* **2** 1201
[11] Saumon D and Chabrier G 1992 *Phys. Rev.* A **46** 2084
[12] Magro W R, Ceperley D M, Pierleoni C and Berm B 1996 *Phys. Rev. Lett.* **76** 1240
[13] Reinholz H, Redmer R and Nagel S 1995 *Phys. Rev.* E **52** 5368
[14] Mott N F 1961 *Phil. Mag.* **6** 287
[15] Nellis W J, Louis A A and Ashcroft N W 1998 *Phil. Trans. R. Soc. Lond.* A **356** 5
[16] Pilgrim W-C, Ross M, Yang L H and Hensel F 1997 *Phys. Rev. Lett.* **78** 3685
[17] Winter R, Bodensteiner T, Gläser W and Hensel F 1987 *Ber. Bunsenges. Phys. Chem.* **91** 1327
[18] Franz G, Freyland W, Gläser W, Hensel F and Schneider E 1980 Structure of expanded liquid rubidium by neutron diffraction *Proc. 4th Int. Conf. on Liquid and Amorphous Metals, J. Physique Coll.* **41** C8 194–8
[19] Pilgrim W-C, Winter R, Hensel F, Morkel C and Gläser W 1995 *Ber. Bunsenges. Phys. Chem.* **95** 1133–6
[20] Copley J R D and Rowe J M 1974 *Phys. Rev. Lett.* **32** 49
[21] Hoshino K, Ugawa H and Watabe J 1992 *J. Phys. Soc. Japan* **61** 2182
[22] Kahl G, Kambayashi S and Nowotny G 1993 *J. Non-Cryst. Solids* **15** 156
[23] Mao H K and Hemley R J 1994 *Rev. Mod. Phys.* **66** 671
[24] Redmer R and Warren W W Jr 1993 *Phys. Rev.* B **48** 14 892
[25] Redmer R, Reinholz H, Röpke G, Winter R, Noll F and Hensel F 1992 *J. Phys.: Condens. Matter* **4** 1659
[26] Smoluchowski R 1967 *Nature* **215** 691
[27] Schouten J A, van den Berg L C and Trappeniers N J 1985 *Chem. Phys. Lett.* **114** 401
[28] van den Bergh L C and Schouten J A 1988 *J. Chem. Phys.* **89** 2336
[29] Stevenson D J 1983 *High Pressure in Science and Technology, Proc. IXth AIRAPT Int. High Pressure Conf.* ed C Homan, R C McCrone and E Whalley (New York: North-Holland) p 357
[30] Klepeis J E, Schafer K J, Barbee T W III and Ross M 1991 *Science* **254** 986
[31] Pfaffenzeller O, Hohl D and Ballone P 1995 *Phys. Rev. Lett.* **74** 2599
[32] Marceca E, Schäfer G and Hensel F 1996 *J. Chem. Thermodynamics* **28** 647
[33] Stevenson D J 1979 *J. Phys. F: Met. Phys.* **9** 791